

## Generation of Ruddlesden-Popper faults in Sr doped NdNiO<sub>3</sub>

Chao Yang<sup>1</sup>, Roberto Ortiz<sup>2</sup>, Yi Wang<sup>3</sup>, Daniel Putzky<sup>2</sup>, Eva Benckiser<sup>3</sup>, Bernhard Keimer<sup>4</sup> and Peter A. van Aken<sup>3</sup>

<sup>1</sup>Max Planck Institute for Solid State Research, Baden-Wurttemberg, Germany, <sup>2</sup>Max Planck Institute for Solid State Research, Germany, <sup>3</sup>Max Planck Institute for Solid State Research, Stuttgart, Germany, Germany, <sup>4</sup>Max Planck Institute for Solid State Research, Stuttgart, Germany, Baden-Wurttemberg, Germany.

\* Corresponding author: [C.Yang@fkf.mpg.de](mailto:C.Yang@fkf.mpg.de); [Y.Wang@fkf.mpg.de](mailto:Y.Wang@fkf.mpg.de)

In the past decades, a great deal of efforts to understand the unconventional high-temperature superconductivity has been focusing on cuprates. Given the similarity between cuprates and nickelates [1, 2], achieving superconductivity in nickelates has attracted considerable attention. Recently, the exciting discovery of superconductivity in hole-doped NdNiO<sub>2</sub> inspires further investigations on nickelates. [3] The infinite-layer NdNiO<sub>2</sub> structure plays a dominated role in nickelate superconductivity, which can be synthesized by an oxygen de-intercalation reaction of Nd<sub>0.8</sub>Sr<sub>0.2</sub>NiO<sub>3</sub> (NSNO) with perovskite structure. [3] However, Ruddlesden-Popper (RP) faults in nickelate films easily occur due to a lattice mismatch with the substrate. These RP faults are electrocatalytically very active sites for the oxygen evolution reaction. [4, 5] Explorations of the role of RP faults are indispensable to understand structure-property correlations in perovskite oxides.

In this study, using aberration-corrected scanning transmission electron microscopy (STEM), we investigate the atomic structure and chemical information of NdNiO<sub>3</sub> (NNO) and Sr-doped Nd<sub>1-x</sub>Sr<sub>x</sub>NiO<sub>3</sub> (NSNO) thin films grown on SrTiO<sub>3</sub> (001) substrate by atomic layer-by-layer MBE, as well as defects inside the thin film. Figure 1(a) shows an HAADF-STEM image of an NSNO film with a thickness of ~ 9 nm. As the contrast of the HAADF image is proportional to  $\sim Z^{1.7}$  (atomic number Z), one can easily distinguish STO and NSNO. The regions marked with red dashed boxes demonstrate three types of RP faults, and the enlargements correspond to boxes A, B, and C, respectively. The RP faults includes a  $\frac{1}{2}$  a  $\langle 111 \rangle$  shift, disappearance of the contrast of A/B sites in the NdNiO<sub>3</sub> structure [5, 6] and single or several intergrowth layers of {NdNiO<sub>3</sub>}.

Figure 2 shows EELS elemental maps of the RP-faults region and the STO/NNO interface. The critical thickness of the (001) perovskite structure of NNO is two unit cells, where Ni and Nd display a distinct contrast corresponding to their elemental maps. With the increase of the film thickness, the contrast differences between Ni and Nd decrease, especially in the right bottom region. The gradual decrease between the Ni and Nd contrast reveals a RP fault with  $\frac{1}{2}$  a  $\langle 111 \rangle$ , demonstrating the intermixing of Ni and Nd. The atomic-resolved EELS elemental maps substantiate the RP-fault formation and interfacial chemistry in nickelates. Furthermore, we will discuss effects of non-stoichiometric elemental ratios (Nd/Ni) and defects at the edge of RP faults on the measured electrostatic field and charge distribution by four-dimensional scanning transmission electron microscopy (4D-STEM).

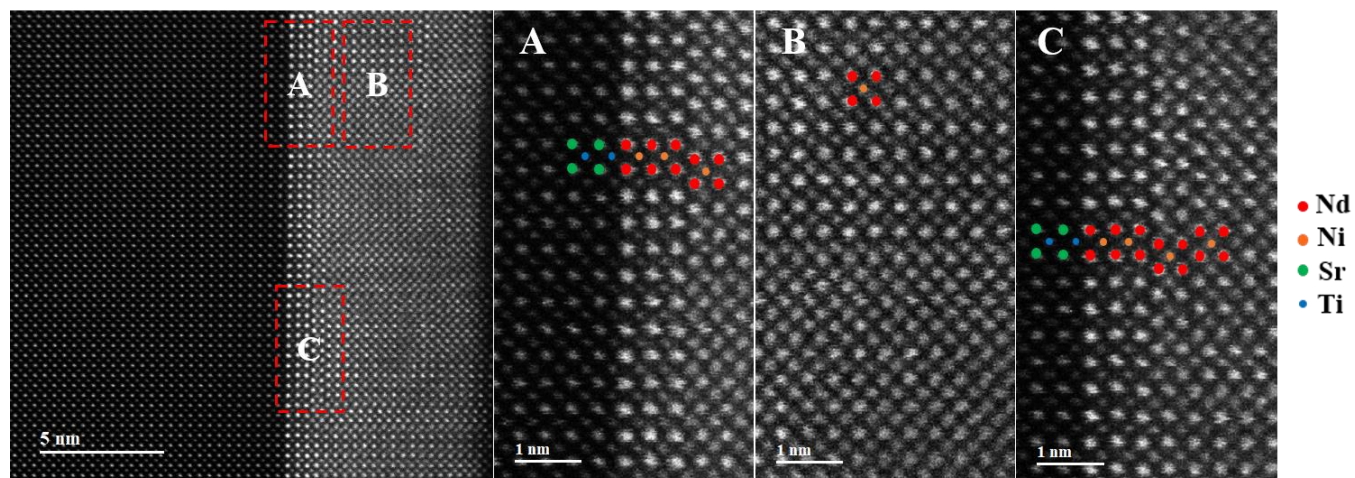


**Figure 1.** Figure 1. HAADF-STEM image of a Nd<sub>0.8</sub>Sr<sub>0.2</sub>NiO<sub>3</sub> thin film grown on a SrTiO<sub>3</sub> substrate. Different types of RP faults: (A) 1/2 a <111> shift, (B) disappearance of contrast of A/B sites, (C) single intergrowth layer of {NdNiO<sub>3</sub>}

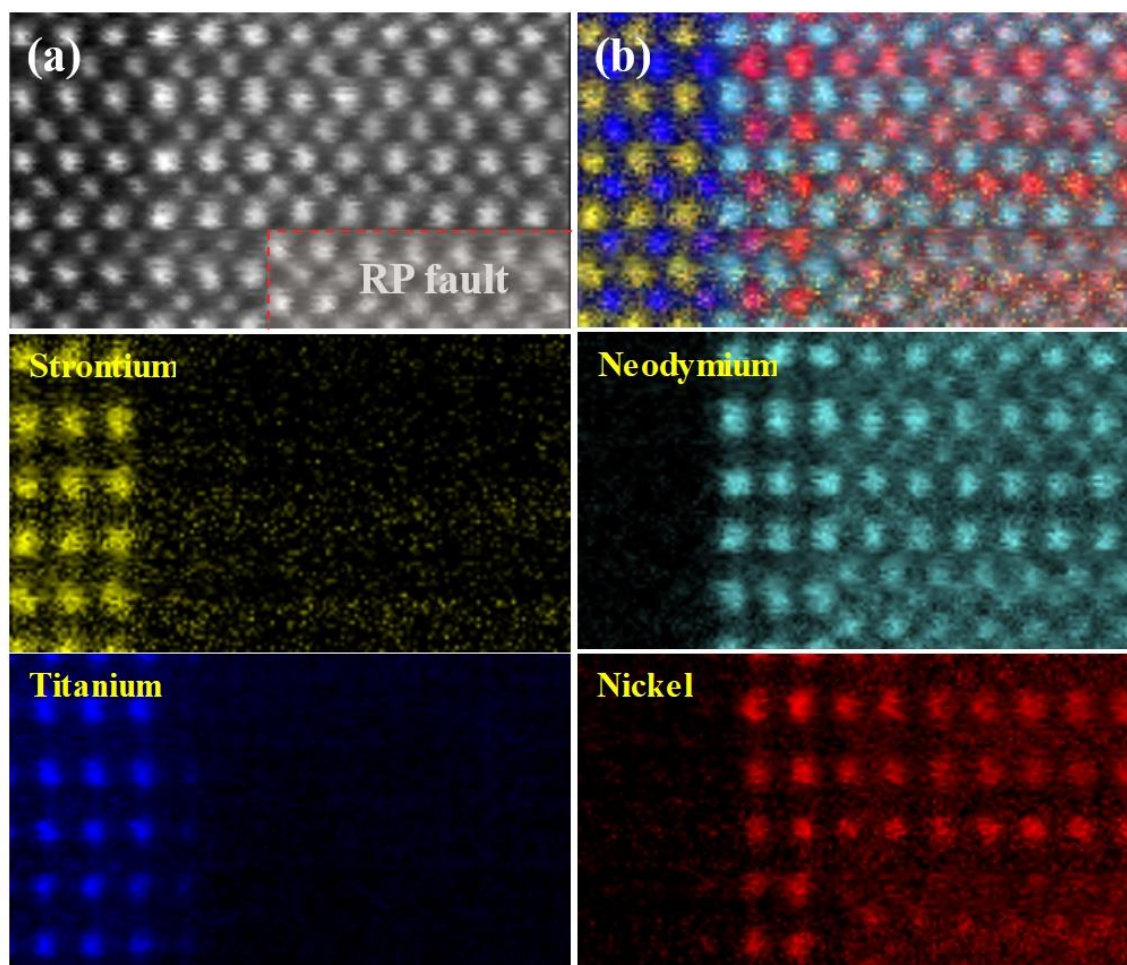


**Figure 2.** Figure 2. STEM-EELS elemental mapping of a RP fault. (a) ADF image of the measured EELS spectrum. (b) The color-coded cation maps for Sr, Ti, Nd and Ni, respectively.

## References

- [1] M Hepting *et al.* Nat. Mater., **19**(4) (2020), p.381-385.
- [2] AS Botana *et al.* Phys. Rev. X **10**(1) (2020), p.011024.
- [3] DF Li *et al.* Nature, **572**(7771), (2019), p.624-627.
- [4] K Lee *et al.* APL Mater., **8**(4) (2020), p.041107.
- [5] J Bak *et al.* Nano Lett., **17**(5) (2020), p.3126-3132.
- [6] C Coll *et al.* J. Phys. Chem. C, **121**(17) (2017), p.9300-9304.